Am J Cancer Res 2024;14(5):2216-2227
www.ajcr.us /ISSN:2156-6976/ajcr0156674

Original Article

MRI monitoring of combined therapy with transcatheter arterial delivery of NK cells and systemic administration of sorafenib for the treatment of HCC

Zigeng Zhang[1*], Guangbo Yu[2*], Aydin Eresen[1,3*], Qiaoming Hou[1], Vahid Yaghmai[1,3], Zhuoli Zhang[1,2,3,4]

[1]Department of Radiological Sciences, University of California Irvine, Irvine, CA, USA; [2]Department of Biomedical Engineering, University of California Irvine, Irvine, CA, USA; [3]Chao Family Comprehensive Cancer Center, University of California Irvine, Irvine, CA, USA; [4]Department of Pathology and Laboratory Medicine, University of California Irvine, Irvine, CA, USA. [*]Equal contributors.

Received March 19, 2024; Accepted April 27, 2024; Epub May 15, 2024; Published May 30, 2024

Abstract: This preclinical study explored the synergistic potential of sorafenib and NK cell chemoimmunotherapy to combat hepatocellular carcinoma (HCC) in a rat model. We aimed to enhance NK cell cytotoxicity through IL-12/18 cytokines supplementation and elucidate the underlying molecular mechanisms driving this collaborative antitumor action. Twenty-four Sprague-Dawley rats were divided into distinct treatment groups, receiving sorafenib via gavage and NK cells via catheterization of the proper hepatic artery. Tumor growth and treatment response were monitored through weekly MRI scans, including T1w, T2w, DCE, and DWI sequences. Histological examinations assessed tumor cell viability, apoptosis fraction, and microvessel density. The combined therapy demonstrated significant inhibition of tumor growth, angiogenesis, and induction of durable antitumor immunity compared to either modality alone. DCE-MRI and DWI revealed distinct alterations in tumor microvasculature, highlighting the effectiveness of the combination. Our findings highlight the promise of sorafenib-augmented NK cell chemoimmunotherapy as a potential therapeutic strategy for HCC management. The targeted delivery of IL-12/18 cytokines supplemented NK cells effectively enhanced cytotoxicity within the tumor microenvironment, leading to improved antitumor responses. Further investigation in clinical trials is warranted to validate these findings in human patients and explore the translational potential of this approach.

Keywords: Combination therapy, hepatocellular carcinoma, immunotherapy, memory-like natural killer cells, sorafenib, therapeutic response

Introduction

Hepatocellular carcinoma (HCC), a highly aggressive malignant disease frequently associated with liver cirrhosis, ranks as the fifth most common cancer globally and the second leading cause of cancer-related deaths worldwide [1, 2]. As hepatectomy, liver transplantation, and ablative therapies offer potential cures for early-stage HCC, most cases are diagnosed at intermediate or advanced stages, rendering these options ineffective. This makes systemic therapy a crucial component of the therapeutic approach for these patients [3].

Sorafenib, the first FDA-approved targeted drug for HCC, is a dual aryl urea multikinase inhibitor targeting cell signaling and angiogenesis [4, 5]. The antitumor action of sorafenib unfolds through two main mechanisms: directly inhibiting tumor cell proliferation via the RAF/MEK/ERK pathway and indirectly suppressing tumor growth by blocking vascular endothelial growth factor receptor (VEGFR) and platelet-derived growth factor receptor (PDGFR), thereby hindering angiogenesis [6]. Consequently, sorafenib has demonstrably improved patient survival rates [7, 8]. However, the widespread use of sorafenib is overshadowed by potential drawbacks. Non-specific uptake by healthy tissues can lead to adverse effects like skin rash, diarrhea, high blood pressure, and hand-foot syndrome [9-11]. Additionally, the emergence of drug resistance poses a growing challenge among patients [5].

https://doi.org/10.62347/IAR01564

Natural killer (NK) cells, effector lymphocytes within the innate immune system, hold immense promise for treating HCC through adoptive transfer immunotherapy (NK-ATI). However, three significant hurdles must be overcome to unlock their full potential [12, 13]. The primary obstacle lies in the inadequate homing efficiency of highly potent NK cells to the tumor site which limits efficiently targeting and eliminating cancerous cells. Moreover, predicting individual patient response to NK-ATI is crucial, yet we lack reliable non-invasive methods. This limitation complicates the identification of individuals benefiting most from this promising therapy [14-16]. Another pivotal factor influencing the efficacy of NK cells in contemporary cancer therapies is NK cell exhaustion. This state is marked by reduced responsiveness and compromised capacity to eliminate tumor cells effectively. A multitude of factors contribute to NK cell exhaustion, such as inhibitory signals emanating from tumor cells, the presence of immunosuppressive cytokines within the tumor microenvironment, and heightened expression of checkpoint molecules that hinder NK cell function. Exploiting the immune memory exhibited by NK cells towards antigens, cytomegalovirus, and cytokines offers a promising avenue to enhance efficacy in response to this challenge [17]. The study of Zwirner and Domaica suggested an enhanced cytotoxicity against hematological malignancies when supplemented with IL-12/15 and IL-18 cytokines in vitro [18]. Additionally, a recent study revealed increased cytotoxic function in NK cells when treated with IL-2 and IL-15 cytokines, combined with cetuximab, targeting HCC cells [19]. Therefore, cytokine activated NK cells (pNK) offer a viable strategy for sustaining enduring NK cell effector functions in vivo.

Recent investigations have revealed that sorafenib primes proinflammatory responses in tumor-associated macrophages (TAMs) within the HCC microenvironment, subsequently enhancing cytotoxic activity in NK cells [20, 21]. This suggests an additional mechanism through which sorafenib may exert anticancer effects, potentially offering novel insights for NK-based immunotherapy. This observation underscores the capacity of sorafenib to enhance the antitumor activity of NK cells in patients with HCC. Thus, sorafenib not only inhibits tumor cell proliferation but also synergistically potentiates the antitumor activity of NK cells, particularly in conjunction with NK-ATI for HCC.

In this study, we aim to evaluate the early treatment response of sorafenib plus catheter delivery of pNK cell immunochemotherapy against HCC by monitoring changes in tumor tissue and tumor perfusion after implantation and treatment in rodent models by MRI.

Materials and methods

In our preclinical studies, we follow the guidelines established by the Institutional Animal Care and Use Committee and treat animals humanely while regularly monitoring the quality of life of the subjects. The framework of the study was visualized in **Figure 1**.

Cell lines and culturing

The N1-S1 rat hepatoma cell line was cultured in Iscove's Modified Dulbecco's Medium (IMDM), supplemented with 10% fetal bovine serum (FBS) (Gibco, Grand Island, NY), 1.25% GlutaMAX (Gibco, Waltham, MA), and 1% penicillin/streptomycin (Gibco, Waltham, MA), following established protocols. The cells were maintained in a controlled environment at 37°C with a humidified atmosphere comprising 5% CO_2 and 95% air. The cells were sub-cultured approximately every three days, and viability measurements were obtained after staining the cells with 0.4% trypan blue dye (Invitrogen, Carlsbad, CA). The cell viability before implantation was ensured to be greater than 90%.

The rat NK cell line, RNK-16, generously provided by Thomas L. Olson (University of Virginia, Charlottesville, VA), was cultured in RPMI medium (Life Technologies, Waltham, MA), supplemented as mentioned earlier, with the addition of 25 mM 2-Mercaptoethanol. Before experimental use, RNK-16 cells underwent treatment with recombinant mouse IL-12 and IL-18 for 24 hours. Subsequently, the cells were washed with PBS and allowed to rest in a fresh medium for an additional 24 hours.

H&E staining

Hematoxylin and eosin (H&E) staining is a widely employed technique in histology for visualizing tissue architecture. Hematoxylin, through its affinity for cations, imparts a positive charge,

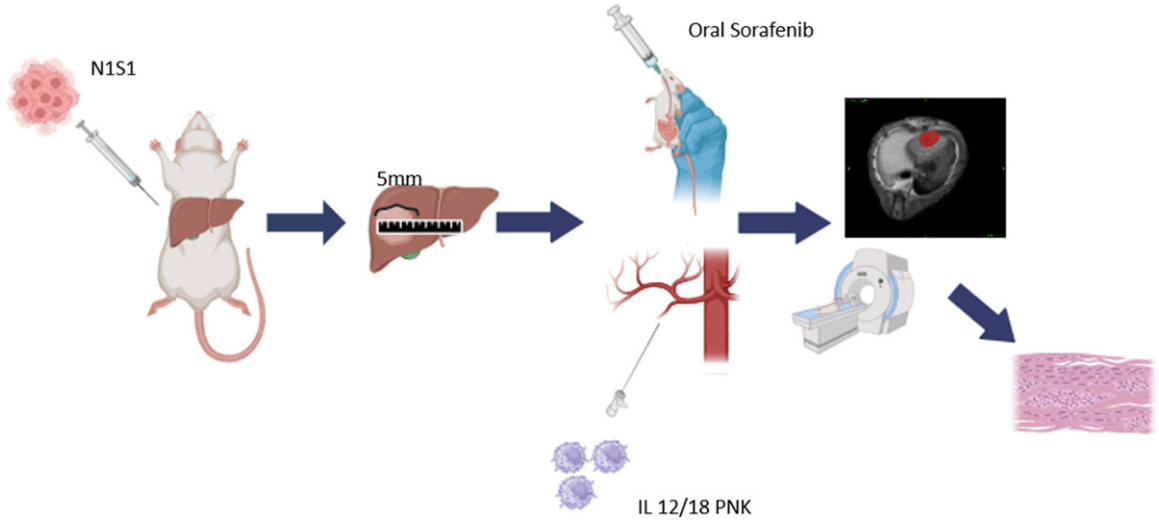

Figure 1. 24 SD rats were all implanted with N1S1 cells and were randomly assigned to 4 different groups and received weekly MRI examinations. When the tumor volume reached 5 mm, rats in the combination group, and control group underwent catheter surgery, and rats in the sorafenib group received sorafenib orally for one week.

facilitating its interaction with negatively charged cellular components, such as nucleic acids within the cell nucleus, resulting in a distinctive purple-blue coloration. Conversely, eosin, possessing an acidic nature and negative charge, binds with positively charged structures like cytoplasmic proteins, yielding the characteristic pink hue observed in the cytoplasm. In healthy, viable cells, uniform staining and regular cellular morphology are typically observed. Consequently, the staining pattern can serve as an indicator of cellular viability. Additionally, during cellular proliferation, the nucleus undergoes enlargement due to chromosome replication. Hence, the abundance of blue-stained cell nuclei can serve as a marker for cellular proliferation capacity.

IACUC approved protocol number

AUP-21-019

Animal model

All experimental procedures involving animals received ethical approval from the Institutional Animal Care and Use Committee at the University of California, Irvine. Twenty-four male Sprague-Dawley (SD) rats were randomly assigned to distinct treatment groups, including a combination group, sorafenib-only group, NK cells-only group, and a control group, with six SD rats allocated to each group. Anesthesia was administered through inhalation of isoflurane according to the guidelines during all procedures and imaging. N1-S1 cells were injected into the largest liver lobe of SD rats. Tumor size was measured using MRI approximately 5-7 days post-implantation and treatment initiation occurred when tumors reached an approximate size of 5 mm.

Gavage and transcatheter infusion

Upon detecting orthotopic liver tumors measuring approximately 5 mm, the treatment initiation for the experimental subjects commenced. In the sorafenib-treatment group, sorafenib tosylate diluted in a 1:1 mixture of castor oil (Kolliphor® EL, Sigma Aldrich, St. Louis, MO) and 95% ethanol was infused using a bulb-tipped gastric feeding needle to the rat's stomach. Sorafenib was administered at a daily dose of 10 mg/kg for 7 days in both the sorafenib treatment and combination treatment groups.

Rats assigned to the NK cell immunotherapy and combination groups underwent a meticulously executed invasive catheterization of the proper hepatic artery. The catheterization procedure involved surgically exposing the portal triad above the initial duodenal loop. Subsequently, a temporary ligation of the common hepatic artery with a 2-0 suture was performed to mitigate the risk of hemorrhage. Simultaneously, a permanent ligation of the

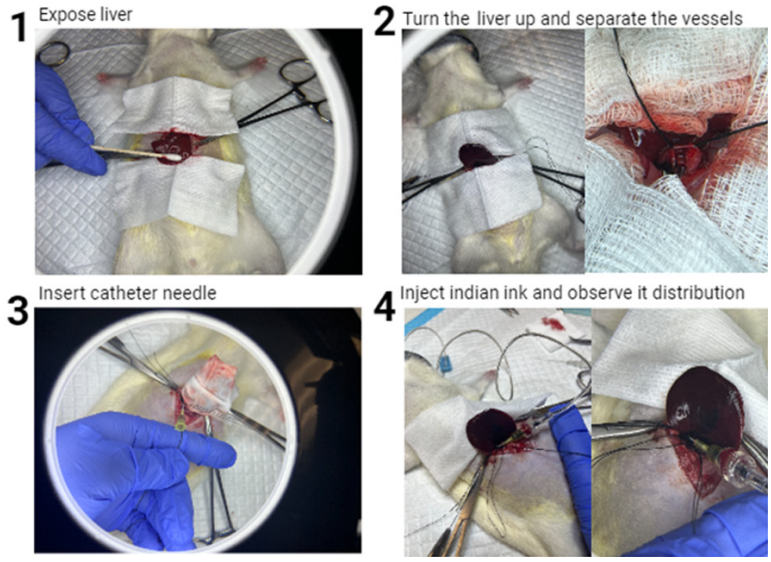

Figure 2. Intrahepatic arterial (IHA) catheterization procedure: Expose liver, separate the vessel and insert catheter needle from GDA to IHA then inject Indian ink. In the real surgery, 0.1 mL of heparin, 4.0 × 10^6 pretreated NK cells (PNK), and 0.3 mL of PBS have been delivered from the IHA to the liver lobes. For the control group, 0.8 mL of PBS was infused, which was equivalent to the volume of the IHA group, and the rest of procedure was performed as same as the IHA group.

gastroduodenal artery was carried out with a 4-0 suture to prevent the retrograde flow of microspheres into the gastrointestinal tract. Following this, a 24G microcatheter (Terumo SurFlash®, Somerset, NJ) was carefully inserted distal to the ligation point in the gastroduodenal artery, guiding it into the proper hepatic artery from the gastroduodenal artery (**Figure 2**). Afterward, 0.1 mL of heparin was infused through the catheter, followed by the administration of 1×10^7 rat NK cells suspended in 0.3 mL PBS with an additional 0.5 mL of PBS. The catheter was then removed, and a 4-0 suture was employed to permanently ligate the gastroduodenal artery proximal to the inoculation site to prevent bleeding. The control group underwent procedures mirroring those of the NK immunotherapy group, with the exception that 1 mL of PBS was infused through the catheter instead of the therapeutic agent.

MRI

MRI scans were performed one week after tumor implantation utilizing a 3T Philips Achieva clinical MRI scanner and a commercially available wrist coil. Anesthesia was induced using 1-2% isoflurane in a mixture of air and oxygen (75/25% vol/vol, 2 L/min). Treatment initiation occurred upon the tumor reaching to diameter of 5 mm. Following this, rats underwent weekly MRI assessments until two weeks post-treatment to monitor tumor growth and evaluate treatment response in vivo. The imaging protocol included diffusion weighted echo planar images with repetition time of 5017 ms, 83 ms echo time, a voxel size of 0.6 mm × 0.6 mm, a slice thickness of 2 mm without inter-slice gap. Additionally, the protocol specified optimized 11 averages, and a maximal field of view (FOV) ranging from 5 cm to 6 cm. All DWI acquisitions employed three b-values (b = 0 s/mm^2 for the T2 component and b = 500/1000 s/mm^2), enabling the calculation of the average diffusion coefficient from pairs of zero and non-zero values.

Upon completion of the MRI image collection, tumor tissues were demarcated utilizing ITK-SNAP (version 4.0), leveraging anatomical (T1 weighted (T1W) and T2-weighted (T2W)), dynamic contrast-enhanced (DCE), and diffusion-weighted imaging (DWI) MRI data. Subsequently, both Python and Graph Prism were employed for visualization and statistical analysis.

Histology

Following the completion of the MRI scan, liver tissues were systematically gathered for subsequent histological examinations, and their sections were meticulously aligned based on the MRI orientation. Typically, one to two sections spanning the identified lesion were procured and then meticulously fixed in a solution containing 10% formalin. Subsequently, these specimens underwent paraffin embedding and were precisely sectioned to a thickness of 5 μm. The processed samples were then dispatched to the Experimental Tissue Shared Resource Facility at the University of California, Irvine, in Orange, CA, for pathological analysis.

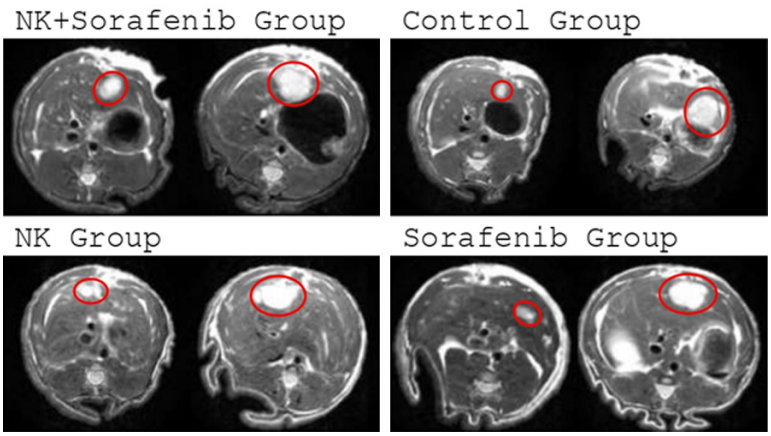

Figure 3. Representative T2w MRI data for the subjects receiving different treatments. In each pair, left image shows the initial size of the tumor and right one is at the end of the study.

Hematoxylin-eosin (H&E) staining was employed to assess both tumor and NK cells, while terminal deoxynucleotidyl transferase dUTP nick end labeling (TUNEL) staining was conducted to evaluate cell apoptosis. Additionally, CD31 staining was performed to examine malignant tumor neovascularization. For CD31 staining, tissue sections underwent standard processing and antigen retrieval. Following a 1-hour block with a 10% BSA and horse serum in PBS, sections were incubated overnight at 4°C with anti-CD31 antibody, appropriately diluted in the blocking solution, within a humidified chamber. After three PBS washes, sections were exposed to a peroxidase-conjugated secondary antibody, succeeded by DAB substrate for immunolabeling, and Mayer's hematoxylin for counterstaining. A pathologist reviewed the histology slides upon the completion of the staining process.

Three quantitative histological measures were determined the number of viable tumor cells from H&E slides, the apoptosis fraction from TUNEL slides, and the microvessel density from CD31 slides. The apoptotic fraction represented the area of apoptosis as a percentage of the total tumor area. For microvessel density measurements, hot spots were identified, and brownish-color endothelial cells or clusters separated from surrounding structures were counted at 200X magnification. These three measurements were independently evaluated by researchers in a minimum of 5 fields per specimen, and the results were subsequently averaged.

Data analysis

The presentation of the data employed various visualization methods, such as box and whisker plots delineating the interquartile range, minimum and maximum values, as well as bars representing the mean ± SEM (standard error of the mean). To analyze the data statistically, a comprehensive suite of tests, including one-way ANOVA and T tests, was executed using GraphPad Prism 7 (version 7.0a, GraphPad Software, Boston, MA). In determining the statistical significance, two-tailed tests were utilized, providing a robust evaluation of the data. The significance levels were delineated as follows: * denoting $P < 0.05$; ** indicating $P < 0.01$; *** representing $P < 0.001$; and **** signifying $P < 0.0001$. This rigorous statistical approach ensured a thorough examination of the data, facilitating precise interpretations and conclusions.

Results

MRI analysis

Five days post-tumor implantation, the rats underwent scanning, during which T1W, T2W, DCE, and DWI were conducted to acquire comprehensive images. HCC tumors were identified under guidance of T1W and T2W MRI data by comparing the signal intensities with liver tissue. **Figure 3** illustrates the clear localization of HCC through a comparative analysis of T2W MR images. The assessment of maximum tumor diameter on T2W MRI indicated an initial tumor size of approximately 5 mm across all groups. Treatment commenced immediately, followed by weekly scans for 2 weeks of post-treatment.

DW-MRI data was acquired to identify heightened cellular density within tumor tissue compared to normal liver tissue. This elevation is indicative of a constricted extracellular space and a higher density of hydrophobic membranes, resulting in impeded diffusion of water protons. Analysis of the acquired images facili-

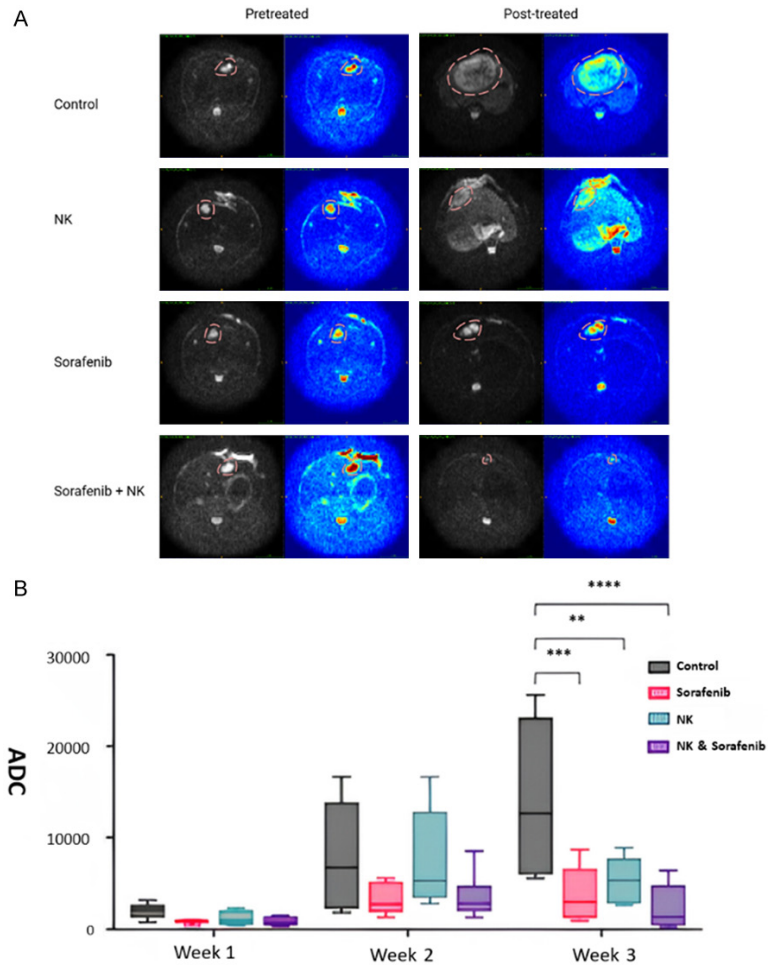

Figure 4. Diffusion weighted images and analysis. A. Representative DWI before and after treatment. Red-dashed lines enclose margins of tumor zone. B. T-test showed that different group has different ΔADCs after treatment (*P < 0.05, **P < 0.01, ***P < 0.001, ****P < 0.0001).

tated the derivation of ΔADC, representing the difference between the ADC of the pretreated and post-treated. In the combined group, the ΔADC value showed a decreased ΔADC (*P < 0.05, **P < 0.01, ***P < 0.001, ****P < 0.0001), which significantly differ from other groups (**Figure 4**).

DCE-MRI is employed to evaluate quantitative and biologically pertinent insights into tumor vasculature and angiogenesis of the HCC tumor under different treatment conditions. A valuable imaging technique that furnishes. **Figure 5A** illustrates the time intensity curve (TIC) of the control group, NK group, sorafenib group, and combination group during DCE-MRI at pre-contrast injection, initial contrast arrival, and contrast plateau. Throughout the initial week (pre-treated phase), no significant differences were observed in the rate and peak signal intensity increase among the groups. However, by the third week (post-treatment phase), the control group exhibited the most pronounced and earliest elevation in tissue signal intensity, reaching a peak and subsequently stabilizing at this level. In contrast, the combined group displayed a gradual increase in tissue signal intensity, with a peak value significantly lower than that of the other groups. The peak tissue signal for the NK group and sorafenib group was notably lower than that of the control group and significantly higher than that of the combination group, with no significant disparity between the NK and sorafenib groups. The area under the TIC was normalized to the baseline signal, and the area under the curve (AUC) was calculated every 30 seconds and averaged across all animals (**Figure 5B**). Consistent with the visual observations in **Figure 5**, the control group exhibited the most substantial intensity increase compared to the combination, NK, and sorafenib groups. Although there was no significant disparity in intensity between the NK group and sorafenib group, both exhibited intensities significantly greater than that in the control group. This indicates that, in comparison to the other groups, the tumor blood supply is notably compromised in the combination group, leading to a significant inhibition of new blood vessel growth.

Histology analysis

The assessment of tumor cell viability involved enumerating viable cells across five distinct regions on randomly selected H&E-stained digital histology slides (**Figure 6A-D**). One-way ANOVA revealed significantly divergent results among the experimental groups (P < 0.05). A

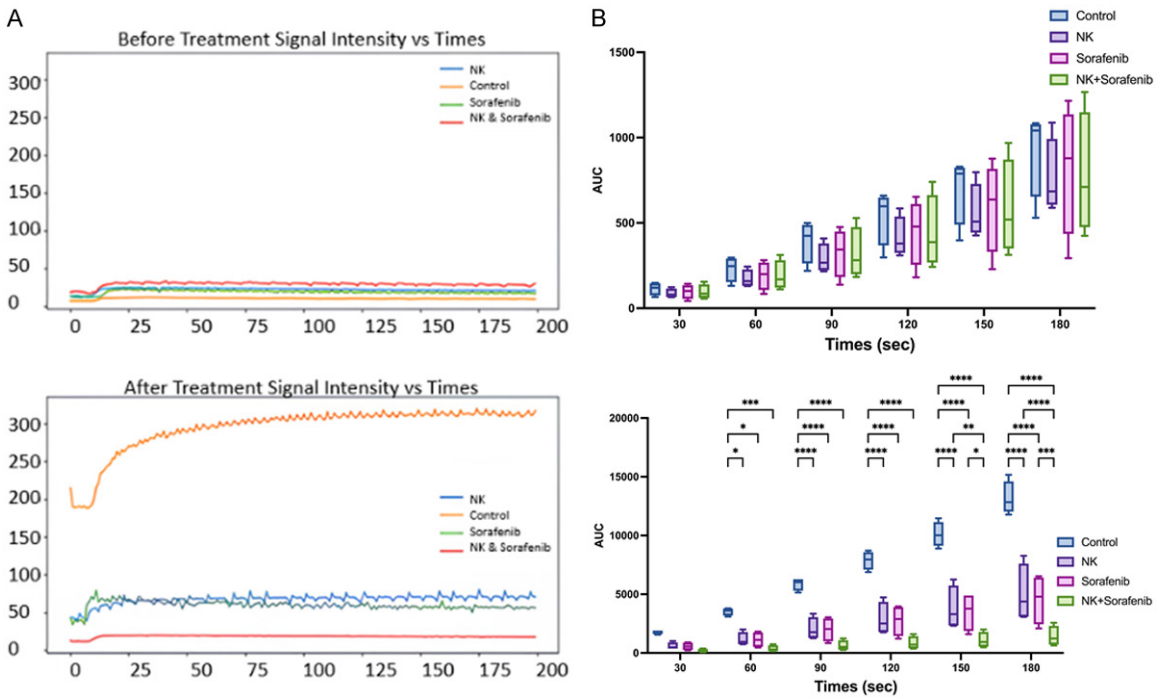

Figure 5. DCE-MRI and analysis of after treatment and before treatment groups. A. Representative TICs of control group, sorafenib group, NK group and sorafenib plus NK group. Representative DCE-MRI images of tumor at 25 s, 100 s, 150 s, are presented below representative TICs. B. Average AUCs of control group, sorafenib group, NK group and sorafenib plus NK group at 30 s, 60 s, 90 s, 120 s, 150 s and 180 s. T-test of AUCs in different groups showed that AUCs are different across groups for all time points ($P < 0.05$).

paired T-test demonstrated that the combined treatment of sorafenib and pNK cell immunotherapy notably facilitated robust cell growth in HCC tumors compared to all other treatment groups ($P < 0.0001$). Notably, the pNK cell group exhibited a more pronounced treatment response than the sorafenib group ($P = 0.027$), despite both groups displaying substantial progression in cell death ($P < 0.001$). Pairwise comparative analysis of tumor survival rates under various treatments further substantiated these findings (**Figure 6E**).

CD31 staining was performed to evaluate the microvessel density within the tumor regions as an indicator of tumor growing pattern. In analysis of the tumor regions, we observed a significantly decreasing ratio of microvessel density following any of the treatments that combined therapy leading the highest effect (1.61%) with least endothelial cell staining (**Figure 6F-I**). The presence of newly formed small blood vessels was evident, distributed throughout the tumor region in the control group (27.29%). Both sorafenib group (8.48%) and NK cell therapies (9.09%) displayed a reduced distribution and a smaller number of these newly formed small blood vessels. Sorafenib treatment led to stronger reduction in microvessel compared to NK cell immunotherapy, yet no significant was reached ($P = 0.91$). The subjects in control group predominantly exhibited a modest positive reaction on CD31, facilitating higher ratio of vessels than treatment groups leading significant changes ($P < 0.02$) (**Figure 6J**).

In sections stained with the TUNEL assay, the combination treatment group exhibited robust overall positive staining for apoptosis (**Figure 6K-N**). Within the tumor area, a substantial extent of cell death was observed, with nearly all cells demonstrating intense positive staining on TUNEL (1.91% apoptosis, **Figure 6O**). In contrast, both the NK cell group and the Sorafenib group displayed a heterogeneous pattern of cells, showing a mix of positive and negative staining on TUNEL (1.16% and 0.94% apoptosis, **Figure 6O**). The control group predominantly exhibited negative staining on TUNEL, with only a limited number of cells per field displaying positive staining at 200X magnification (0.49% apoptosis, **Figure 6O**). Despite

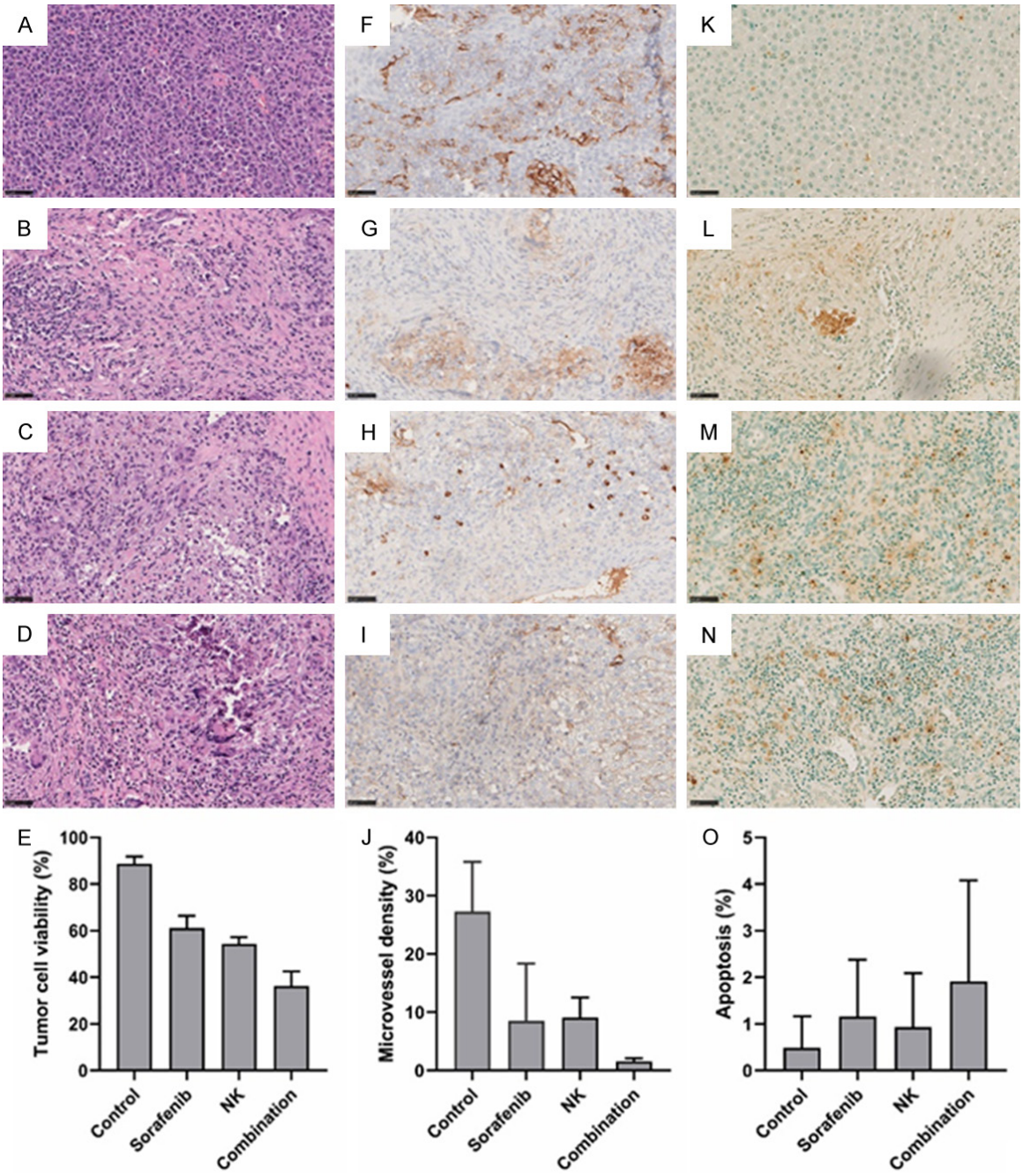

Figure 6. Histologic analysis of tumor tissues. HE-stained (A-D), CD31-stained (F-I), TUNEL-stained (K-N) representative cross sections of tumor tissue after different treatment, with 400× magnification views of each treatment region and for each stain. (E) Tumor cell viability index of each group's tumor. (J) Microvessel density index of each group's tumor. (O) Apoptotic index of each group's tumor.

the strong difference between the groups, a significance was not able to be observed which may be indirectly affected by the tumor cell viability with H&E staining. Notably, the combination treatment group demonstrated the highest level of apoptosis, followed by Sorafenib and NK treatment groups, and finally, control group.

Discussion

Currently a range of clinically utilized drugs for HCC treatment, including bevacizumab, Lenvatinib, and cisplatin. However, these pharmaceuticals still harbor limitations. Bevacizumab, a monoclonal antibody targeting vascular endothelial growth factor (VEGF), poses significant

risks of adverse reactions such as bleeding, hypertension, proteinuria, and gastrointestinal perforation. While it can impede tumor growth by targeting angiogenesis, its efficacy as a standalone agent in HCC treatment may be constrained compared to combination therapies [22]. Lenvatinib, a multikinase inhibitor, is associated with side effects such as hypertension, proteinuria, diarrhea, and fatigue, potentially compromising patients' quality of life. Moreover, the development of resistance over time diminishes its efficacy as a viable treatment option [23]. Cisplatin, a chemotherapy agent, is notorious for its nephrotoxic effects, leading to kidney damage [24]. Its mechanism of action impacts both malignant and healthy cells, resulting in severe side effects like nausea, vomiting, and bone marrow suppression. In contrast, NK cell therapy leverages the body's immune system to selectively target cancer cells, offering the promise of a more focused and sustained anti-tumor response. Furthermore, when combined with sorafenib, NK cell therapy engenders a synergistic effect that amplifies the overall efficacy of the treatment.

In our study, we focused on the synergistic effects of these modified NK cells in conjunction with sorafenib treatment against HCC tumor cells, assessing their efficacy through MRI and histological analysis. We cultured NK cells from rat NK cell line and pretreated them with IL-12 and IL-18 cytokines to increase the efficacy against HCC tumors. Twenty-four male SD rats implanted with N1-S1 tumor cells were given sorafenib, pretreated NK cell or combined treatment respectively. Our findings demonstrated that the combination therapy outperformed individual treatments, significantly increasing HCC tumor cell death. Moreover, the combined therapy effectively suppressed early tumor growth, with visible results observed within the initial seven days of treatment.

In line with the current Barcelona Clinic Liver Cancer (BCLC) staging system, sorafenib stands as a crucial treatment option for patients grappling with intermediate and advanced HCC. Nonetheless, sorafenib falls short of perfection. Its administration typically elongates median survival time by a mere 3 months, and the array of side effects often compels patients to either scale back on dosage or discontinue usage altogether [25]. Our study endeavors to augment sorafenib's efficacy while mitigating these drawbacks. Noteworthy research reveals sorafenib's capacity to modulate various immune cells within the HCC tumor microenvironment (TME), particularly enhancing NK cell function at lower doses without inducing exhaustion [26]. Moreover, NK cells play a pivotal role in the body's immune surveillance, exhibiting no discernible cytotoxicity towards normal cells. This insight propels our investigation towards the amalgamation of NK cell therapy with sorafenib treatment.

Certain studies have noted limited effectiveness in transferring NK cells, potentially linked to prolonged tumor exposure [27]. To tackle this challenge, researchers have explored the use of cytokine-induced preconditioned NK cells, albeit predominantly in hematologic cancers rather than liver cancer. Asakawa et al. proposed a potential involvement of IL-18 and its receptor in constitutive activation [28]. Additionally, there's evidence supporting IL-12's capacity to enhance antigen presentation and improve tumor cell targeting [29, 30]. Our study focuses on assessing the viability of utilizing IL-12 and IL-18 pretreated NK cells in conjunction with sorafenib against HCC tumor cells.

In current preclinical investigations, multiphase CT or MRI serve as the primary tools for monitoring. CT is favored for its accessibility and thorough examination of the chest and abdomen [31]. MRI boasts greater sensitivity, particularly in T2W images, which delineate normal tissue as hypointense regions, while highlighting viable tumors as hyperintense [32]. Treatment-induced necrosis may lead to a lack of enhancement in subsequent imaging, hence the preference for MRI to avoid potential interference from CT. Among imaging techniques, DWI is notable for its ability to accurately quantify tumor necrosis post-treatment. DCE images offer a visual representation of tumor blood supply. Our focus was on correlating MRI findings with histological outcomes. Consistently, our experimental data demonstrate the effectiveness of MRI in monitoring tumor treatment, providing a non-invasive means for assessing therapeutic response.

Conclusions

This study investigated the synergistic antitumor potential of combination sorafenib plus

pNK cell chemoimmunotherapy and targeted delivery techniques for the treatment of HCC. Our findings suggest that this multifaceted approach holds significant promise for overcoming current limitations and improving therapeutic outcomes in HCC patients. To address the homing limitation, we employed transcatheter IHA infusion of pNK cells directly into the liver tissue. This targeted delivery strategy facilitated efficient pNK cell infiltration, enabling them to strategically accumulate around and directly engage with tumor cells. Furthermore, pretreatment of NK cells with IL-12 and IL-18 enhanced their cytotoxic potential, thereby amplifying their antitumor capacity. For the purpose of tumor detection, our study employed MRI imaging modalities, specifically T2W, DCE, and DWI, to assess tumor growth and functional characteristics. After data acquisition, histological analysis was undertaken. The concordance observed between the histological findings and those derived from MRI underscores the potential of MRI as a non-invasive modality for HCC monitoring.

However, our experiments faced certain limitations. Sorafenib, while effective, comes with significant side effects, including skin reactions, diarrhea, fatigue, hypertension, and potential blood and liver toxicity. These adverse reactions may necessitate dosage adjustments or even discontinuation, which can severely impact the treatment's effectiveness. Regrettably, in our experiments, monitoring and managing these side effects were not feasible. The duration of our drug administration, lasting only one week, was insufficient for significant side effects to manifest. Nevertheless, previous research has outlined strategies for handling such side effects. The primary approach involves adjusting the sorafenib dosage based on the severity of adverse events (AEs), following BCLC recommendations. Tailored strategies are employed for each type of adverse event. Diarrhea requires immediate intervention to mitigate its severity and maintain treatment efficacy. Management primarily focuses on symptom relief, hydration, electrolyte balance, and patient education regarding dietary modifications and the use of antidiarrheal medications like loperamide. Hand-foot skin reaction which typically resolves upon discontinuing sorafenib [33].

Despite the challenges posed by limitations, the transition of our experimental findings into clinical application remains highly feasible. This feasibility is underpinned by the FDA approval of both Sorfenib and IL-12 as clinical drugs, along with the extensive utilization of IL-18 in numerous preclinical studies [34, 35]. While our experiments utilized rat NK cell line, it is worth noting that the FDA has approved NK-92 as a clinical drug [36]. Although further efforts may be required to facilitate the translation into clinical practice, the prospects for such transition remain promising.

Acknowledgements

This study was supported by the National Cancer Institute of the National Institutes of Health under award numbers R01CA209886, R01CA241532, P30CA062203, Society of Interventional Radiology Foundation, and the University of California Irvine Anti-Cancer Challenge Pilot grant.

Disclosure of conflict of interest

None.

Address correspondence to: Drs. Zhuoli Zhang and Aydin Eresen, Department of Radiological Sciences, School of Medicine, University of California Irvine, 839 Health Sciences Road, Irvine, CA 92617, USA. Tel: 949-824-7820; E-mail: zhuoliz1@hs.uci.edu (ZLZ); Tel: 949-824-1283; E-mail: aeresen@hs.uci.edu (AE)

References

[1] Villanueva A. Hepatocellular carcinoma. N Engl J Med 2019; 380: 1450-1462.

[2] GBD 2015 Mortality and Causes of Death Collaborators. Global, regional, and national life expectancy, all-cause mortality, and cause-specific mortality for 249 causes of death, 1980-2015: a systematic analysis for the Global Burden of Disease Study 2015. Lancet 2016; 388: 1459-1544.

[3] Dimitroulis D, Damaskos C, Valsami S, Davakis S, Garmpis N, Spartalis E, Athanasiou A, Moris D, Sakellariou S, Kykalos S, Tsourouflis G, Garmpi A, Delladetsima I, Kontzoglou K and Kouraklis G. From diagnosis to treatment of hepatocellular carcinoma: an epidemic problem for both developed and developing world. World J Gastroenterol 2017; 23: 5282-5294.

[4] Choi KJ, Baik IH, Ye SK and Lee YH. Molecular targeted therapy for hepatocellular carcinoma:

present status and future directions. Biol Pharm Bull 2015; 38: 986-991.
[5] Zhu YJ, Zheng B, Wang HY and Chen L. New knowledge of the mechanisms of sorafenib resistance in liver cancer. Acta Pharmacol Sin 2017; 38: 614-622.
[6] Pinto E, Pelizzaro F, Farinati F and Russo FP. Angiogenesis and hepatocellular carcinoma: from molecular mechanisms to systemic therapies. Medicina (Kaunas) 2023; 59: 1115.
[7] Palazzo A, Iacovelli R and Cortesi E. Past, present and future of targeted therapy in solid tumors. Curr Cancer Drug Targets 2010; 10: 433-461.
[8] Iacovelli R, Sternberg CN, Porta C, Verzoni E, de Braud F, Escudier B and Procopio G. Inhibition of the VEGF/VEGFR pathway improves survival in advanced kidney cancer: a systematic review and meta-analysis. Curr Drug Targets 2015; 16: 164-170.
[9] Cheng AL, Kang YK, Chen Z, Tsao CJ, Qin S, Kim JS, Luo R, Feng J, Ye S, Yang TS, Xu J, Sun Y, Liang H, Liu J, Wang J, Tak WY, Pan H, Burock K, Zou J, Voliotis D and Guan Z. Efficacy and safety of sorafenib in patients in the Asia-Pacific region with advanced hepatocellular carcinoma: a phase III randomised, double-blind, placebo-controlled trial. Lancet Oncol 2009; 10: 25-34.
[10] Mancuso A, Airoldi A, Vigano R and Pinzello G. Fatal gastric bleeding during sorafenib treatment for hepatocellular carcinoma recurrence after liver transplantation. Dig Liver Dis 2011; 43: 754.
[11] Li M, Su Y, Zhang F, Chen K, Xu X, Xu L, Zhou J and Wang W. A dual-targeting reconstituted high density lipoprotein leveraging the synergy of sorafenib and antimiRNA21 for enhanced hepatocellular carcinoma therapy. Acta Biomater 2018; 75: 413-426.
[12] Lee JH, Lee JH, Lim YS, Yeon JE, Song TJ, Yu SJ, Gwak GY, Kim KM, Kim YJ, Lee JW and Yoon JH. Adjuvant immunotherapy with autologous cytokine-induced killer cells for hepatocellular carcinoma. Gastroenterology 2015; 148: 1383-1391, e1386.
[13] Yu R, Yang B, Chi X, Cai L, Liu C, Yang L, Wang X, He P and Lu X. Efficacy of cytokine-induced killer cell infusion as an adjuvant immunotherapy for hepatocellular carcinoma: a systematic review and meta-analysis. Drug Des Devel Ther 2017; 11: 851-864.
[14] Cheng M, Chen Y, Xiao W, Sun R and Tian Z. NK cell-based immunotherapy for malignant diseases. Cell Mol Immunol 2013; 10: 230-252.
[15] Meier R, Golovko D, Tavri S, Henning TD, Knopp C, Piontek G, Rudelius M, Heinrich P, Wels WS and Daldrup-Link H. Depicting adoptive immunotherapy for prostate cancer in an animal model with magnetic resonance imaging. Magn Reson Med 2011; 65: 756-763.
[16] Jha P, Golovko D, Bains S, Hostetter D, Meier R, Wendland MF and Daldrup-Link HE. Monitoring of natural killer cell immunotherapy using non-invasive imaging modalities. Cancer Res 2010; 70: 6109-6113.
[17] Poznanski SM, Lee AJ, Nham T, Lusty E, Larché MJ, Lee DA and Ashkar AA. Combined stimulation with interleukin-18 and interleukin-12 potently induces interleukin-8 production by natural killer cells. J Innate Immun 2017; 9: 511-525.
[18] Zwirner NW and Domaica CI. Cytokine regulation of natural killer cell effector functions. Biofactors 2010; 36: 274-288.
[19] Mahgoub S, Abosalem H, Emara M, Kotb N, Maged A and Soror S. Restoring NK cells functionality via cytokine activation enhances cetuximab-mediated NK-cell ADCC: a promising therapeutic tool for HCC patients. Mol Immunol 2021; 137: 221-227.
[20] Kamiya T, Chang YH and Campana D. Expanded and activated natural killer cells for immunotherapy of hepatocellular carcinoma. Cancer Immunol Res 2016; 4: 574-581.
[21] Sprinzl MF, Reisinger F, Puschnik A, Ringelhan M, Ackermann K, Hartmann D, Schiemann M, Weinmann A, Galle PR, Schuchmann M, Friess H, Otto G, Heikenwalder M and Protzer U. Sorafenib perpetuates cellular anticancer effector functions by modulating the crosstalk between macrophages and natural killer cells. Hepatology 2013; 57: 2358-2368.
[22] Fang P, Hu JH, Cheng ZG, Liu ZF, Wang JL and Jiao SC. Efficacy and safety of bevacizumab for the treatment of advanced hepatocellular carcinoma: a systematic review of phase II trials. PLoS One 2012; 7: e49717.
[23] Wang S, Wang Y, Yu J, Wu H and Zhou Y. Lenvatinib as first-line treatment for unresectable hepatocellular carcinoma: a systematic review and meta-analysis. Cancers (Basel) 2022; 14: 5525.
[24] Oh GS, Kim HJ, Shen A, Lee SB, Khadka D, Pandit A and So HS. Cisplatin-induced kidney dysfunction and perspectives on improving treatment strategies. Electrolyte Blood Press 2014; 12: 55-65.
[25] Hoechst B, Voigtlaender T, Ormandy L, Gamrekelashvili J, Zhao F, Wedemeyer H, Lehner F, Manns MP, Greten TF and Korangy F. Myeloid derived suppressor cells inhibit natural killer cells in patients with hepatocellular carcinoma via the NKp30 receptor. Hepatology 2009; 50: 799-807.
[26] Eresen A, Pang Y, Zhang Z, Hou Q, Chen Z, Yu G, Wang Y, Yaghmai V and Zhang Z. Sorafenib plus memory like natural killer cell combina-

tion therapy in hepatocellular carcinoma. Am J Cancer Res 2024; 14: 344-354.
[27] Gill S, Vasey AE, De Souza A, Baker J, Smith AT, Kohrt HE, Florek M, Gibbs KD Jr, Tate K, Ritchie DS and Negrin RS. Rapid development of exhaustion and down-regulation of eomesodermin limit the antitumor activity of adoptively transferred murine natural killer cells. Blood 2012; 119: 5758-5768.
[28] Asakawa M, Kono H, Amemiya H, Matsuda M, Suzuki T, Maki A and Fujii H. Role of interleukin-18 and its receptor in hepatocellular carcinoma associated with hepatitis C virus infection. Int J Cancer 2006; 118: 564-570.
[29] Lasek W, Zagożdżon R and Jakobisiak M. Interleukin 12: still a promising candidate for tumor immunotherapy? Cancer Immunol Immunother 2014; 63: 419-435.
[30] Lu X. Impact of IL-12 in cancer. Curr Cancer Drug Targets 2017; 17: 682-697.
[31] Omata M, Lesmana LA, Tateishi R, Chen PJ, Lin SM, Yoshida H, Kudo M, Lee JM, Choi BI, Poon RT, Shiina S, Cheng AL, Jia JD, Obi S, Han KH, Jafri W, Chow P, Lim SG, Chawla YK, Budihusodo U, Gani RA, Lesmana CR, Putranto TA, Liaw YF and Sarin SK. Asian Pacific Association for the Study of the Liver consensus recommendations on hepatocellular carcinoma. Hepatol Int 2010; 4: 439-474.
[32] Guan YS, Sun L, Zhou XP, Li X and Zheng XH. Hepatocellular carcinoma treated with interventional procedures: CT and MRI follow-up. World J Gastroenterol 2004; 10: 3543-3548.
[33] Pang Y, Eresen A, Zhang Z, Hou Q, Wang Y, Yaghmai V and Zhang Z. Adverse events of sorafenib in hepatocellular carcinoma treatment. Am J Cancer Res 2022; 12: 2770-2782.
[34] Lang L. FDA approves sorafenib for patients with inoperable liver cancer. Gastroenterology 2008; 134: 379.
[35] Markowitz GJ, Yang P, Fu J, Michelotti GA, Chen R, Sui J, Yang B, Qin WH, Zhang Z, Wang FS, Diehl AM, Li QJ, Wang H and Wang XF. Inflammation-dependent IL18 signaling restricts hepatocellular carcinoma growth by enhancing the accumulation and activity of tumor-infiltrating lymphocytes. Cancer Res 2016; 76: 2394-2405.
[36] Bergman H, Sissala N, HÄgerstrand H and Lindqvist C. Human NK-92 cells function as target cells for human NK cells - implications for CAR NK-92 therapies. Anticancer Res 2020; 40: 5355-5359.